The Journal of Chemical Physics

Photoelectron imaging of cryogenically cooled BiO^- and BiO_2^- anions

Cite as: J. Chem. Phys. **157**, 171101 (2022); https://doi.org/10.1063/5.0127877
Submitted: 24 September 2022 • Accepted: 17 October 2022 • Accepted Manuscript Online: 17 October 2022 • Published Online: 01 November 2022

G. Stephen Kocheril, Han-Wen Gao, Dao-Fu Yuan, et al.

AIP Publishing

The Journal of Chemical Physics COMMUNICATION scitation.org/journal/jcp

Photoelectron imaging of cryogenically cooled BiO^- and BiO_2^- anions

Cite as: J. Chem. Phys. **157**, 171101 (2022); doi: 10.1063/5.0127877
Submitted: 24 September 2022 • Accepted: 17 October 2022 •
Published Online: 1 November 2022

G. Stephen Kocheril, Han-Wen Gao, Dao-Fu Yuan, and Lai-Sheng Wang[a)]

AFFILIATIONS

Department of Chemistry, Brown University, Providence, Rhode Island 02912, USA

[a)]**Author to whom correspondence should be addressed:** lai-sheng_wang@brown.edu

ABSTRACT

The advent of ion traps as cooling devices has revolutionized ion spectroscopy as it is now possible to efficiently cool ions vibrationally and rotationally to levels where truly high-resolution experiments are now feasible. Here, we report the first results of a new experimental apparatus that couples a cryogenic 3D Paul trap with a laser vaporization cluster source for high-resolution photoelectron imaging of cold cluster anions. We have demonstrated the ability of the new apparatus to efficiently cool BiO^- and BiO_2^- to minimize vibrational hot bands and allow high-resolution photoelectron images to be obtained. The electron affinities of BiO and BiO_2 are measured accurately for the first time to be 1.492(1) and 3.281(1) eV, respectively. Vibrational frequencies for the ground states of BiO and BiO_2, as well as those for the anions determined from temperature-dependent studies, are reported.

I. INTRODUCTION

Ever since its inception in 1981 by Smalley and co-workers, the laser vaporization supersonic cluster source has dominated the field of cluster science as an efficient and robust means of cluster production.[1] Virtually any solid material can be vaporized to form a cluster beam, which is ideal for both mass spectrometry and spectroscopy.[2] However, cluster temperatures are difficult to control in general in a laser vaporization cluster source and they can depend on many factors, such as the geometry of the nozzle, carrier gas, laser vaporization power, and cluster size.[3] Clusters not sufficiently cooled internally present many experimental challenges for spectroscopic experiments, making it difficult to perform high-resolution studies. Cooling cluster anions is particularly challenging because of their relatively low abundance and complicated mechanisms of formation in the laser vaporization cluster source.[3,4]

Cooling molecules has been approached from many directions in the past, but the most effective cooling method for molecular ions has been cryogenic ion trapping. The concept was first demonstrated by Gerlich with his 22-pole ion trap, designed to investigate ion–molecule reactions at low temperatures.[5] The 22-pole ion trap has been widely used in spectroscopic studies of molecular ions.[6–10] Using cryogenic cooling of molecular anions for photoelectron spectroscopy (PES) studies was first demonstrated by our group in 2005 with the temperature-dependent study to observe C–H···O hydrogen bonding involving unactivated alkanes and vibrational cooling of C_{60}^- in a 3D Paul trap.[11–13] Linear ion traps have also been utilized recently to cool cluster anions for PES studies.[14–17] The cryogenically cooled 3D Paul trap is convenient to implement and particularly conducive to ion extraction and subsequent mass analyses.[13] Thus, it has been widely used in different spectroscopy experiments now, in particular for ions from electrospray ionization.[18–27] In recent years, several experimental apparatuses have also been developed to couple a laser vaporization cluster source to a cryogenically cooled ion trap, including both linear and 3D ion trap configurations.[15–17,27–29] These recent developments have further highlighted the importance of active cooling of molecular and cluster ions using ion trap technologies and their impact on spectroscopy. We have been developing a new apparatus that couples our existing laser vaporization supersonic cluster source and velocity map imaging (VMI) system[30] with a cryogenically cooled 3D Paul trap that we originally developed to couple with an electrospray ionization source.[13] Here, we report our initial results on two bismuth oxide anions (BiO^- and BiO_2^-), which are used as testing systems.

The bismuth oxide anions are excellent systems to test our new apparatus since they can be readily produced from our laser vaporization cluster source, yet no PES study on these anions has been done previously. Furthermore, both systems are expected to

have low vibrational frequencies due to the presence of a heavy atom, making them particularly suitable for testing vibrational cooling in our new apparatus. Early spectroscopic information on BiO was summarized in the Huber and Herzberg book on constants of diatomic molecules.[31] There have been a number of further studies on the spectroscopy and electronic structure of BiO.[32–38] The electron affinities (EAs) of BiO and BiO_2 were estimated to be 156 ± 14 and 311 ± 27 kJ/mol, respectively, through thermodynamic measurements.[39] However, there have been no spectroscopic studies on BiO_2, although there have been several mass spectrometric reports on large $Bi_xO_y^+$ cluster cations.[40–44]

In this Communication, we report the first PES study of cold BiO^- and BiO_2^- using photoelectron imaging (PEI) and our newly built cryogenic 3D Paul trap coupled to a laser vaporization cluster source. Vibrationally resolved photoelectron spectra are measured for both anions and the EAs of BiO and BiO_2 are measured accurately to be 1.492(1) and 3.281(1) eV, respectively. Vibrational frequencies for the ground states of BiO and BiO_2, as well as those for the anions determined from temperature-dependent studies, are obtained. Vibrational cooling is demonstrated, opening new opportunities to conduct high resolution PEI studies of size-selected clusters from the laser vaporization cluster source.

II. EXPERIMENTAL METHODS

The experiments were carried out on a newly modified high-resolution photoelectron imaging apparatus equipped with a cryogenically controlled 3D Paul trap, details of which are to be published. The PEI apparatus with the laser vaporization cluster source has been reported in detail previously.[30] In the new version of the instrument, a cryogenically cooled 3D Paul trap[13,21] is inserted between the cluster source and the time-of-flight (TOF) mass spectrometer. Briefly, the second harmonic of a Nd:YAG laser was focused onto a bismuth disk target (99.9% purity, Alfa Aesar). The laser-induced plasma was quenched by a high pressure He carrier gas, seeded with 1% O_2 to promote the formation of bismuth oxide clusters. Nascent clusters were entrained by the carrier gas and underwent a supersonic expansion. Following a skimmer, anions in the collimated beam were sent directly into the cryogenically cooled 3D Paul trap. The ion trap was cooled by a two-stage closed-cycle helium refrigerator down to 4.2 K and could be controlled up to 300 K. The trapped anions were collisionally cooled by a mixed He/H_2 buffer gas (19:1 by volume) for 45 ms before being pulsed into the extraction zone of a TOF mass spectrometer at a 10 Hz repetition rate. The BiO^- and BiO_2^- anions of interest were mass-selected before entering the interaction zone of the velocity map imaging (VMI) lens. Photodetachment was performed using the third harmonic of an injection-seeded Nd:YAG laser (Continuum Powerlite 9020; 355 nm; 3.496 eV) or a YAG-pumped dye laser. Photoelectrons were extracted and focused onto a set of microchannel plates coupled to a phosphor screen and charge-coupled device camera. Raw images were acquired for 100 000–300 000 laser shots and were processed using the maximum entropy Legendre expansion method (MELEXIR).[45] The VMI lens was calibrated using PE images of Au^- and Bi^- at various photon energies. The typical resolution of our VMI system was ~0.6% for high kinetic energy electrons and as low as 1.2 cm^{-1} for very slow electrons.[30] Uncertainties were estimated by measuring at least three independent PE images per photon energy and taking the average of each set of observed spectral features.

PE angular distributions (PADs) were obtained from the images, characterized by the anisotropy parameter (β). The differential cross section of the photoelectrons can be expressed as

$$d\sigma/d\Omega = \sigma_{Tot}/4\pi[1 + \beta P_2(\cos(\theta)], \quad (1)$$

where σ_{Tot} is the total cross section, P_2 is the second-order Legendre polynomial, and θ is the angle of the photoelectrons relative to the laser polarization. Hence, the PAD is described by

$$I(\theta) \sim [1 + \beta P_2(\cos(\theta)], \quad (2)$$

where β has a value ranging from −1 to 2.[46] This model works for single photon detachment transitions from randomly oriented molecules. As photons carry one unit of angular momentum, the angular momentum of the outgoing photoelectron will be $l = \pm 1$. If an electron is detached from an s atomic orbital ($l = 0$), the outgoing photoelectron will have $l = 1$ (pure p-wave) with $\beta = 2$. It is non-trivial to interpret the β-value for electron detachment from molecular orbitals (MOs) since the MOs are linear combinations of atomic orbitals. Nevertheless, the values of β can be used to qualitatively assess the symmetries of the MOs involved in the photodetachment process and provide valuable electronic information.[47]

III. RESULTS AND DISCUSSION

The addition of the ion trap has significantly altered the observed cluster distributions from our laser vaporization source. Previously, the entire anion cluster beam was perpendicularly extracted down the TOF tube, producing a mass spectrum that covered a broad mass range.[3,30] The Paul trap, however, can only trap a limited mass range determined by the radio frequency (RF) voltage due to the different kinetic energies of the anions in the supersonic cluster beam. Furthermore, after the ions were extracted out of the

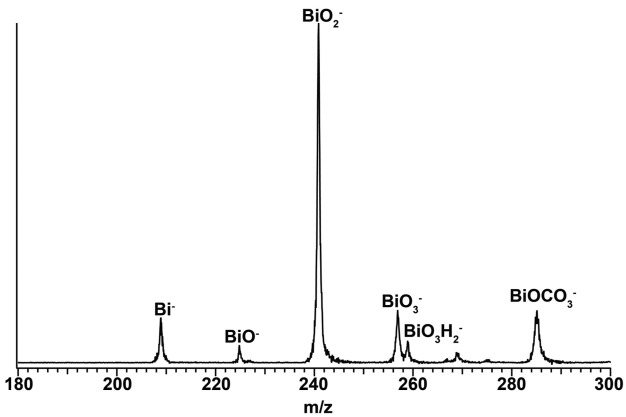

FIG. 1. The mass spectrum of BiO_x^- (x = 0–3) anions produced from a laser vaporization cluster source and cooled in a 3D cryogenic ion trap.

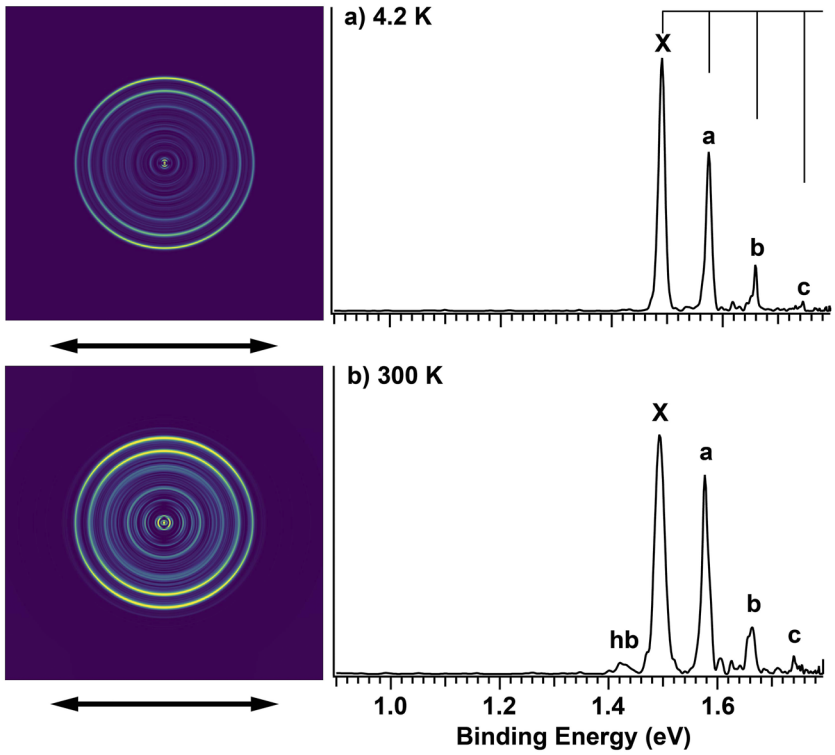

FIG. 2. The photoelectron images and spectra of BiO^- taken at 690.8 nm (1.795 eV) with the ion trap operated at (a) 4.2 K and (b) 300 K. The double arrow below each image indicates the laser polarization.

trap, they began to separate spatially according to their mass-to-charge ratios. Thus, the full range of the trapped ions could not be extracted into the TOF mass spectrometer. Figure 1 displays a mass spectrum for the BiO_x^- (x = 0–3) anions optimized around BiO_2^-, which was by far the most intense anion observed in this mass range. The diatomic BiO^- was significantly weaker in comparison and was also less intense than the Bi^- anion. In this mass range, we also observed BiO_3^- and $BiOCO_3^-$. The latter should be due to trace carbon impurities in the bismuth target. Interestingly, we also observed $BiO_3H_2^-$, which was likely due to chemical reactions between BiO_3^- and H_2 in the thermalization buffer gas. Apparently, no other anions in this mass range were reactive with H_2 in the cold ion trap.

A. Photoelectron imaging of cold BiO^-

Figure 2(a) presents the PE spectrum of cryogenically cooled BiO^- taken at 690.8 nm (1.795 eV) when the ion trap was operated at 4.2 K. The spectrum is very simple with a single vibrational progression corresponding to the Bi–O stretching vibration, representing the detachment transition from the ground state of the BiO^- anion to that of neutral BiO. The 0-0 transition defined by peak X gives rise to an accurate EA of BiO of 1.492 ± 0.001 eV. The X peak has a linewidth of ~10 meV (~80 cm^{-1}) mainly due to the instrumental resolution. The experiment was repeated three times with careful and independent calibration. The scatter of the peak positions was within 1 meV, which defines the experimental uncertainty. Peaks *a*, *b*, and *c* are due to vibrational excitations of BiO (Table I), yielding a vibrational frequency of 675 ± 8 cm^{-1}. BiO^- has a $^3\Sigma^-$ ground state with a half-filled π^* highest occupied molecular orbital (HOMO), giving rise to a $^2\Pi$ ground state for neutral BiO. The observed transition should correspond to the $^2\Pi_{1/2}$ ground spin–orbit state, whereas the $^2\Pi_{3/2}$ spin–orbit excited state is known to be at a substantially higher energy.[35–37] The observed binding energies of the four vibrational peaks of the $^2\Pi_{1/2}$ ground state are summarized in Table I, where the β parameter of each peak is also given. The (s + d)-wave angular distribution is consistent with the detachment of a π^* electron.

We also obtained the PE image and spectrum of BiO^- at 300 K for comparison, as shown in Fig. 2(b). A vibrational hot band was clearly observed, yielding a vibrational frequency of 596 ± 10 cm^{-1} for the BiO^- anion. The reduced vibrational frequency in the anion agrees with the anti-bonding nature of its HOMO. To determine the vibrational temperature of the ions, we performed

TABLE I. The observed binding energies of the vibrational peaks and their β values from the PE spectrum of cold BiO^-.

Peak	Assignment	Binding energy (eV)	ΔE (cm^{-1})[a]	β
hb[b]	v′ = 1	1.421(1)	−596(10)	⋯
X	v = 0	1.492(1)	0	−0.5
a	v = 1	1.576(1)	678(5)	−0.4
b	v = 2	1.660(1)	677(8)	−0.5
c	v = 3	1.743(1)	669(9)	−0.4

[a]Vibrational spacing.
[b]Measured from the 300 K spectrum.

TABLE II. Summary of the molecular constants for BiO and BiO^-.

	BiO ($^2\Pi_{1/2}$)		BiO^- ($^3\Sigma^-$)
	Current work	Literature[a]	Current work
ω_e (cm^{-1})		691.64	
ν (cm^{-1})[b]	675 ± 8	678.32	596 ± 10
$\omega_e x_e$ (cm^{-1})		1.4651	
r_e (Å)		1.934[c]	1.996

[a]From Ref. 37.
[b]Fundamental vibrational frequency.
[c]From Ref. 31.

Franck–Condon (FC) simulations using the PESCAL program with the Morse potential.[48] This was accomplished by manually adjusting the bond length of the anion from the known value of the neutral[31] using the experimentally derived vibrational frequencies. The vibrational temperature of the simulation was adjusted iteratively to best fit the observed vibrational hot band. The best fit is shown in Fig. S1(a), which yielded a bond length increase of 0.062 Å for the anion. This result is also consistent with the stronger Bi–O bond in the neutral because of the anti-bonding nature of the π^* HOMO of BiO^-. A summary of the derived molecular constants for BiO and BiO^- from the FC simulations is given in Table II. We were unable to determine the vibrational temperature from the cold spectrum because the hot band was negligible. The FC simulation at 300 K indeed agrees well with the measured spectrum at a trap temperature of 300 K [Fig. S1(b)], indicating that the BiO^- anions were generally thermalized with the surroundings at this trap temperature.

B. Photoelectron imaging of cold BiO_2^-

Figure 3(a) shows the PE image and spectrum of cryogenically cooled BiO_2^- at 3.496 eV when the Paul trap was operated at 4.2 K. The spectrum, which should be due to the detachment transition from the ground state of BiO_2^- to that of BiO_2, was more complicated because multiple vibrational modes were active. The observed vibrational features and their assignments are summarized in Table III. Peak X is due to the 0-0 transition, defining the EA of BiO_2 to be 3.281 ± 0.001 eV. Peaks *a* and *b* form a short vibrational progression, which should be due to the bending mode (ν_2) with an observed frequency of 140 ± 8 cm^{-1}. The assignments of the weak higher binding energy vibrational peaks were assisted by FC simulations (*vide infra*). We were also able to determine the β parameters of the two intense peaks X and *a*, as given in Table III. The *p*-wave distribution suggests that the HOMO of BiO_2^- should be a σ-type orbital. Surprisingly, there is one weak peak observed below the EA at 3.254 ± 0.002 eV, due to a vibrational hot band derived from the bending mode of BiO_2^-. To confirm the hot band, we also conducted the experiment at a trap temperature of 300 K, as shown in Fig. 3(b). The bending hot band was observed to increase significantly, in addition to the appearance of more unresolved hot bands on the lower binding energy side. The spectrum at 300 K also underlines the importance of cooling anions with low frequency vibrational modes: the bending progression is completely obscured in the 300 K spectrum due to both rotational and vibrational broadening.

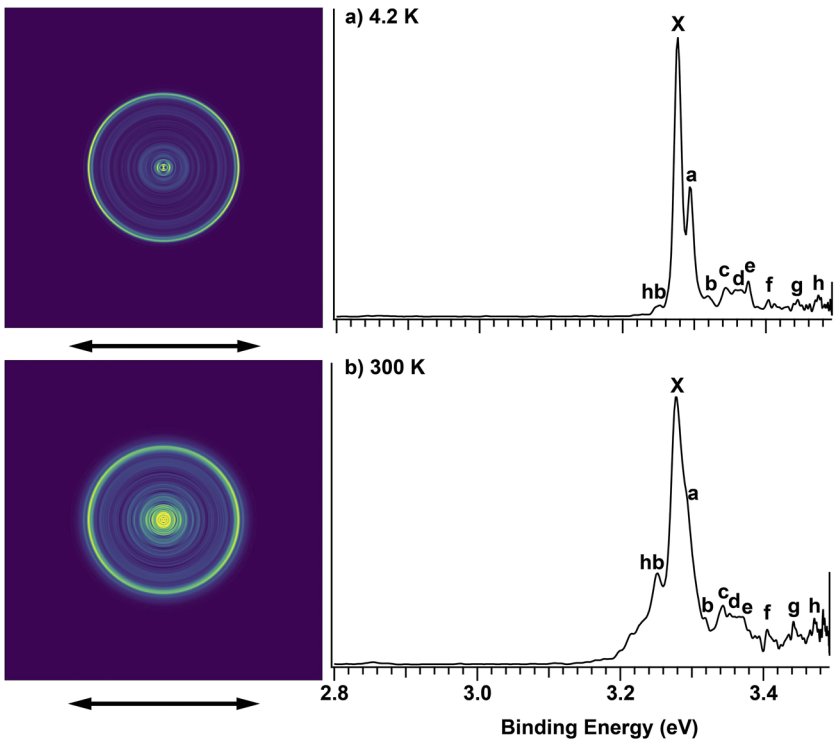

FIG. 3. The photoelectron images and spectra of BiO_2^- taken at 3.496 eV with the ion trap operated at (a) 4.2 K and (b) 300 K. The double arrow below each image indicates the laser polarization.

TABLE III. The experimental binding energies, assignments, and β parameters for the observed vibrational features from the PE spectra of cold BiO_2^-.

Peak	Assignment	Binding energy (eV)[a]	β[a]
hb	2_1^0	3.254(2)	...
X	0_0^0	3.281(1)	0.3
a	2_0^1	3.298(1)	0.1
b	2_0^2	3.318(1)	...
c	3_0^2	3.343(8)	...
d	$2_0^1 3_0^2$	3.359(5)	...
e	1_0^1	3.378(1)	...
f	3_0^4	3.409(2)	...
g	$3_0^2 1_0^1$	3.447(1)	...
h	1_0^2	3.475(2)	...

[a]In cases where the intensity of a transition is too low, the β parameter could not be evaluated properly.

To help understand the observed vibrational features, we carried out FC simulations for BiO_2^-, as shown in Fig. S2(a). The multi-mode FC simulations were performed using the ezFCF suite.[49] There have been no theoretical calculations on BiO_2, but its structure is expected to be bent similar to other group VA dioxides, such as NO_2^- and SbO_2^-.[50–52] Our observation of a low frequency bending mode is also consistent with a bent BiO_2^- and BiO_2. The ground state of BiO_2^- is assumed to be $^1A_1$ and that of BiO_2 to be $^2A_1$, similar to their lighter MO_2^- congeners.[49–52] During the simulation, the initial geometry of the anion was set using the structures of the known group VA dioxides as guides, while the geometry of neutral BiO_2 was manually adjusted from this initial anion geometry to obtain the best fit to the observed spectrum. This process was repeated until the simulation agreed with the experimental observations, using the observed bending vibrational frequencies as a guide. The best fit yielded a bond length change of −0.020 Å and a bond angle change of +4° from the anion to the neutral, as shown in Table IV, where the final anion and neutral structural parameters are also given. These data would be interesting to be compared with future theoretical calculations. We note that a much larger bond angle change was predicted from SbO_2^- to SbO_2, resulting in a broad bending progression in the simulated PE spectrum for SbO_2^-.[52] The FC simulation allowed the weak higher vibrational features to be readily assigned. Peaks *c* and *f* are assigned to the v = 2 and 4 levels of the asymmetric stretch mode (ν_3), which are allowed by symmetry. Peak *d* is assigned as the combination of the overtone of the asymmetric stretch and the bending mode, while peak *g* is assigned to the combination of the overtone of the asymmetric stretch and the symmetric stretch (ν_1). These three transitions allow us to estimate the asymmetric stretch frequency to be 270 cm^{-1} with a large uncertainty (Table IV). Peaks *e* and *h* are assigned to the symmetric stretching mode, giving rise to a vibrational frequency of 789 ± 8 cm^{-1}. The obtained spectroscopic constants for BiO_2 and BiO_2^- are summarized in Table IV.

TABLE IV. Molecular constants for BiO_2 and BiO_2^- from the current work.

	BiO_2 ($^2A_1$)	BiO_2^- ($^1A_1$)
ν_1 (cm^{-1})	789 ± 8	...
ν_2 (cm^{-1})	140 ± 8	215 ± 8
ν_3 (cm^{-1})	270 ± 40	...
Δr_e (Å)	−0.020 [anion (1.995) → neutral (1.975)]	
$\Delta\theta$ (deg)	+4 [anion (108) → neutral (112)]	

We were able to estimate the vibrational temperature of the cooled BiO_2^- anions using the FC simulation and the vibrational hot band of the bending mode. According to the simulation, the 2_1^0 hot band was not clearly populated until T_{vib} ~ 80 K, which seemed to be rather high. Previously, we were able to achieve rotational temperatures for trapped anions of about 30–35 K in the 3D Paul trap from anions produced from an electrospray source.[53,54] We expected that the vibrational temperature should be similar. However, it was possible that the rotational and vibrational temperatures were not in equilibrium. It is also possible that we did not find the optimal cooling conditions yet for the newly designed ion trap because we were focusing on obtaining the best trapping efficiency for each ion. The buffer gas pressure and composition, RF amplitude, trapping time, and possible collisional heating during ion extraction from the Paul trap could all influence the final observed vibrational temperature.[13]

The FC simulation of the 300 K spectrum [Fig. S2(b)] indicates that the vibrational temperature of BiO_2^- was roughly in equilibrium with the ion trap at this temperature. Despite the incomplete vibrational cooling of BiO_2^- at 4.2 K, the cold spectrum was still a huge improvement in comparison to the 300 K spectrum. Without the ion trap, we expected that the supersonic cooling would not be able to cool the BiO_2^- anion down to 80 K to allow the well-resolved spectrum shown in Fig. 3(a). We were able to obtain a T_{vib} of only 175 K for Au_2^- previously from the supersonic cluster source.[4] We are still tuning and optimizing the newly designed ion trap system. We expect to be able to determine both rotational and vibrational temperatures using suitable anions.

IV. CONCLUSIONS

We have demonstrated vibrational cooling using a temperature-controlled 3D Paul trap for anions produced from a laser vaporization cluster source. The addition of the cryogenic Paul trap has allowed us to significantly quench vibrational hot bands that are present when clusters are formed by laser vaporization but are difficult to cool during the supersonic expansion. Test experiments were done on cryogenically cooled BiO^- and BiO_2^-, allowing us to determine both the electron affinities as well as the vibrational structures of BiO and BiO_2 for the first time. The current study has shown that we can trap and cool molecular anions from a laser vaporization cluster source using a temperature-controlled 3D Paul trap, which should open new possibilities to study cluster anions using high resolution photoelectron imaging.

SUPPLEMENTARY MATERIAL

See the supplementary material for the Franck–Condon simulations for the photoelectron spectra of BiO^- and BiO_2^-.

ACKNOWLEDGMENTS

This work was supported by the National Science Foundation (Grant No. CHE-2053541). G.S.K. would like to thank NASA RISG for partial support (Grant No. 80NSSC20M0053).

AUTHOR DECLARATIONS

Conflict of Interest

The authors have no conflicts to disclose.

Author Contributions

G. Stephen Kocheril: Conceptualization (equal); Data curation (lead); Formal analysis (lead); Funding acquisition (supporting); Writing (co-lead). **Han-Wen Gao**: Data curation (supporting); Writing (supporting). **Dao-Fu Yuan**: Data curation (supporting); Writing (supporting). **Lai-Sheng Wang**: Conceptualization (equal); Formal analysis (supporting); Funding acquisition (lead); Writing (co-lead).

DATA AVAILABILITY

The data that support the findings of this study are available within the article and its supplementary material and are available from the corresponding author upon reasonable request.

REFERENCES

[1] T. G. Dietz, M. A. Duncan, D. E. Powers, and R. E. Smalley, J. Chem. Phys. **74**, 6511 (1981).
[2] M. A. Duncan, Rev. Sci. Instrum. **83**, 041101 (2012).
[3] L. S. Wang, Int. Rev. Phys. Chem. **35**, 69 (2016).
[4] I. León, Z. Yang, and L.-S. Wang, J. Chem. Phys. **138**, 184304 (2013).
[5] D. Gerlich, Adv. Chem. Phys. **82**, 1 (1992).
[6] T. R. Rizzo, J. A. Stearns, and O. V. Boyarkin, Int. Rev. Phys. Chem. **28**, 481 (2009).
[7] R. Wester, J. Phys. B: At., Mol. Opt. Phys. **42**, 154001 (2009).
[8] S. Chakrabarty, M. Holz, E. K. Campbell, A. Banerjee, D. Gerlich, and J. P. Maier, J. Phys. Chem. Lett. **4**, 4051 (2013).
[9] A. Günther, P. Nieto, D. Müller, A. Sheldrick, D. Gerlich, and O. Dopfer, J. Mol. Spectrosc. **332**, 8 (2017).
[10] O. Asvany and S. Schlemmer, Phys. Chem. Chem. Phys. **23**, 26602 (2021).
[11] X.-B. Wang, H.-K. Woo, B. Kiran, and L.-S. Wang, Angew. Chem., Int. Ed. **44**, 4968 (2005).
[12] X.-B. Wang, H.-K. Woo, and L.-S. Wang, J. Chem. Phys. **123**, 051106 (2005).
[13] X.-B. Wang and L.-S. Wang, Rev. Sci. Instrum. **79**, 073108 (2008).
[14] C. Bartels, C. Hock, J. Huwer, R. Kuhnen, J. Schwöbel, and B. von Issendorff, Science **323**, 1323 (2009).
[15] C. Hock, J. B. Kim, M. L. Weichman, T. I. Yacovitch, and D. M. Neumark, J. Chem. Phys. **137**, 244201 (2012).
[16] M. L. Weichman and D. M. Neumark, Annu. Rev. Phys. Chem. **69**, 101 (2018).
[17] R. Tang, X. Fu, and C. Ning, J. Chem. Phys. **149**, 134304 (2018).
[18] A. B. Wolk, C. M. Leavitt, E. Garand, and M. A. Johnson, Acc. Chem. Res. **47**, 202 (2014).
[19] C. M. Choi, D. H. Choi, N. J. Kim, and J. Heo, Int. J. Mass Spectrom. **314**, 18 (2012).
[20] I. Alata, J. Bert, M. Broquier, C. Dedonder, G. Feraud, G. Grégoire, S. Soorkia, E. Marceca, and C. Jouvet, J. Phys. Chem. A **117**, 4420 (2013).
[21] L.-S. Wang, J. Chem. Phys. **143**, 040901 (2015).
[22] B. M. Marsh, J. M. Voss, and E. Garand, J. Chem. Phys. **143**, 204201 (2015).
[23] S.-i. Ishiuchi, H. Wako, D. Kato, and M. Fujii, J. Mol. Spectrosc. **332**, 45 (2017).
[24] D. H. Kang, S. An, and S. K. Kim, Phys. Rev. Lett. **125**, 093001 (2020).
[25] C. Kjaer, J. Langeland, T. T. Lindkvist, E. R. Sorensen, M. H. Stockett, H. C. Kjaergaard, and S. B. Nielsen, Rev. Sci. Instrum. **92**, 033105 (2021).
[26] S. J. P. Marlton and A. J. Trevitt, Chem. Commun. **58**, 9451 (2022).
[27] J. T. Buntine, E. Carrascosa, J. N. Bull, U. Jacovella, M. I. Cotter, P. Watkins, C. Liu, M. S. Scholz, B. D. Adamson, S. J. P. Marlton, and E. J. Bieske, Rev. Sci. Instrum. **93**, 043201 (2022).
[28] M. D. Johnston, W. L. Pearson, G. Wang, and R. B. Metz, Rev. Sci. Instrum. **89**, 014102 (2018).
[29] E. K. Campbell and P. W. Dunk, Rev. Sci. Instrum. **90**, 103101 (2019).
[30] I. León, Z. Yang, H.-T. Liu, and L.-S. Wang, Rev. Sci. Instrum. **85**, 083106 (2014).
[31] K. P. Huber and G. Herzberg, *Molecular Spectra and Molecular Structure. IV. Constants of Diatomic Molecules* (Van Nostrand Reinhold Company, New York, 1979).
[32] I. Mayo, J. Bachar, S. Rosenwaks, F. Martin, R. Bacis, and J. Verges, J. Chem. Phys. **93**, 7923 (1990).
[33] E. H. Fink, K. D. Setzer, D. A. Ramsay, and M. Vervloet, Chem. Phys. Lett. **179**, 103 (1991).
[34] F. Martin, R. Bacis, C. Linton, J. Vergès, I. Mayo, and S. Rosenwaks, J. Chem. Phys. **95**, 255 (1991).
[35] C. Linton, R. Bacis, F. Martin, S. Rosenwaks, and J. Vergès, J. Chem. Phys. **96**, 3422 (1992).
[36] A. B. Alekseyev, H. P. Liebermann, R. J. Buenker, G. Hirsch, and Y. Li, J. Chem. Phys. **100**, 8956 (1994).
[37] O. Shestakov, R. Breidohr, H. Demes, K. D. Setzer, and E. H. Fink, J. Mol. Spectrosc. **190**, 28 (1998).
[38] E. A. Cohen, D. M. Goodridge, K. Kawaguchi, E. H. Fink, and K. D. Setzer, J. Mol. Spectrosc. **239**, 16 (2006).
[39] O. V. Kuznetsova, V. I. Semenkhin, E. B. Rudnyi, and L. N. Sidorov, Zh. Fiz. Khim. SSSR **66**, 3160 (1992).
[40] H. Struyf, L. Van Vaeck, and R. Van Grieken, Rapid Commun. Mass Spectrom. **10**, 551 (1996).
[41] M. Kinne, T. M. Bernhardt, B. Kaiser, and K. Rademann, Int. J. Mass Spectrom. **167–168**, 161 (1997).
[42] M. R. France, J. W. Buchanan, J. C. Robinson, S. H. Pullins, J. L. Tucker, R. B. King, and M. A. Duncan, J. Phys. Chem. A **101**, 6214 (1997).
[43] M. J. Van Stipdonk, D. R. Justes, R. D. English, and E. A. Schweikert, J. Mass Spectrom. **34**, 677 (1999).
[44] J. Optiz-Coutureau, A. Feilicke, B. Kaiser, and K. Rademann, Phys. Chem. Chem. Phys. **3**, 3034 (2001).
[45] B. Dick, Phys. Chem. Chem. Phys. **21**, 19499 (2019).
[46] J. Cooper and R. N. Zare, J. Chem. Phys. **48**, 942 (1968).
[47] A. Sanov and R. Mabbs, Int. Rev. Phys. Chem. **27**, 53 (2008).
[48] K. M. Ervin, PESCAL, Fortran program, 2010.
[49] S. Gozem and A. I. Krylov, Wiley Interdiscip. Rev.: Comput. Mol. Sci. **12**, e1546 (2021).
[50] K. M. Ervin, J. Ho, and W. C. Lineberger, J. Chem. Phys. **92**, 5405–5412 (1988).
[51] E. P. F. Lee, J. M. Dyke, F.-T. Chau, W.-K. Chow, and D. K. W. Mok, J. Chem. Phys. **125**, 064307 (2006).
[52] E. P. F. Lee, J. M. Dyke, D. K. W. Mok, F.-T. Chau, and W.-K. Chow, J. Chem. Phys. **127**, 094306 (2007).
[53] H.-T. Liu, C.-G. Ning, D.-L. Huang, and L.-S. Wang, Angew. Chem., Int. Ed. **53**, 2464 (2014).
[54] D.-L. Huang, G.-Z. Zhu, and L.-S. Wang, J. Chem. Phys. **142**, 091103 (2015).